

Conversion of the Bruker Minispec Instrumentation into the Static Magnetic Field Standard

Peter Andris*, Ivan Frollo, Jiří Přibíl, Daniel Gogola, Tomáš Dermek

Institute of Measurement Science, Slovak Academy of Sciences, Dubravská cesta 9, 841 04 Bratislava, Slovakia, peter.andris@savba.sk

Abstract: The static magnetic field standard is part of many scientific experiments aimed at measuring the magnetic field. Often this device has to be built by oneself, if there is no possibility to buy it off the shelf. One possibility is also to convert a suitable device into a static magnetic field standard. Such a method is also described in this article. When the first experiments showed that the key parts could not be obtained under the existing conditions, it was decided to convert Bruker's Minispec into a static magnetic field standard. Such a standard will not be completely universal, but it will accommodate many experiments, and the experience may help in the future when a more perfect standard is built. This article describes the design of the apparatus, briefly describing all the equipment, which includes many parts of the original device. The parts specific to the new construction are described in more detail. An alternative solution for frequency deviation calculation using a software quadrature detector, tested only in the form of a computer simulation, is also described.

Keywords: Bruker Minispec, static magnetic field standard, permanent magnet, NMR magnetometer, complex signal.

1. INTRODUCTION

Standards for static magnetic fields are constructed in different ways. After testing various components for the construction of the standard, we decided to use a variant based on the redesigned Bruker Minispec pc 100. The main component of interest was a permanent magnet with magnetic field stabilization circuits. Minispec has performed some tasks with nuclear magnetic resonance (NMR) circuits, some of which were used in the construction of the standard. It can be said that the standard consists of the circuits of a magnet and an NMR magnetometer. The circuitry of the magnet was mostly taken from Minispec, the magnetometer was mostly constructed at our workplace. The NMR signal receiver was partially adopted, the signal processing is original. The signal is obtained as an even function of frequency; the sign of the signal is additionally determined with a logical algorithm. However, computer simulation also tested signal processing by quadrature detection, which provides the signal as an odd function of frequency. In this case, the frequency deviation sign does not have to be determined additionally. The signal processing method will be selected after long-term testing of the device. The article briefly describes the theory used and how it can be applied to the proposed construction. Most of the theory is derived from the Fourier transform [1], [2]. Reference [3] describes one of our earliest constructions. Verification experiments revealed that the electromagnet used is not suitable for use with nuclear magnetic resonance,

although other circuits can be used. Therefore, we switched from this variant to a permanent magnet from Minispec. Article [4] describes the design of a magnetometer based on NMR. The magnetometer in this article is very similar to our magnetometer design, of course its working conditions are completely different from ours. Article [5] is a review publication on NMR magnetometers. It contains information suitable both for the designer and for a beginner who wants to understand the principles of such an apparatus. In article [6], experienced metrology experts describe the standard of a static magnetic field with an NMR magnetometer using the NMR phenomenon with running water. The authors of [7], [8] present some principles of NMR science. Research of the authors [9] aims at the application of this science. Similarly, the authors [10]-[13] present their works based on the application of the NMR technique. The authors [14] reflect on the importance and roles of measurement for science in general.

2. SUBJECT & METHODS

The described static magnetic field standard was created by modifying the Minispec pc 100 device from Bruker. A permanent magnet and some electronic circuits were used. Fig. 1 shows a simplified block diagram of the standard. The standard according to this scheme consists of two main circuits. It is the circuit of a permanent magnet and the circuit of an NMR magnetometer.

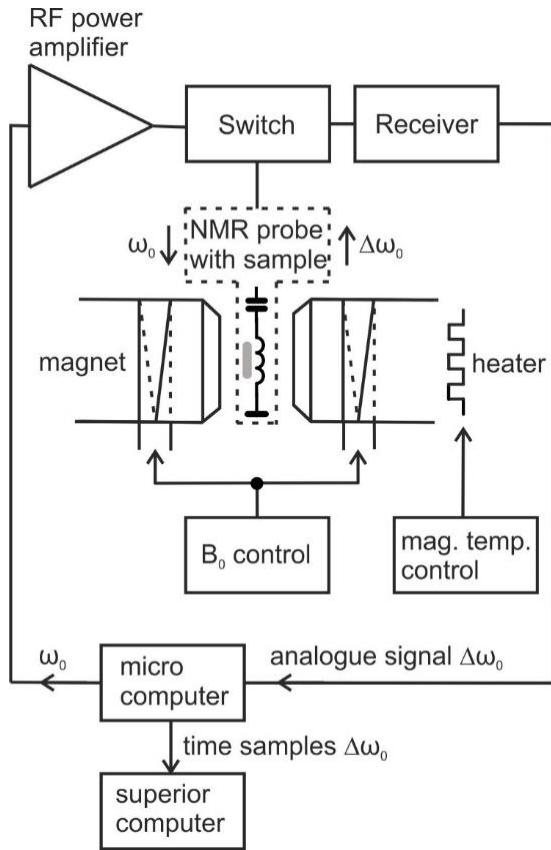


Fig. 1. Block diagram of the static magnetic field standard.

Permanent magnet circuit

The magnet is of type "C" with two pole attachments. Small coils are wound on the attachments. They are powered by direct current and serve for fine-tuning of the resulting magnetic field B_0 . The adjusting element is a potentiometer and is accessible from the outside without disassembling the instrument. The magnetic field of a permanent magnet also depends on its temperature, so the magnet is heated while its temperature is stabilized at 38 °C. The stability of the magnetic field can be increased with a stabilizer. The stabilizer can be controlled by the signal from an NMR magnetometer, but this signal is discontinuous, which complicates its use. Therefore, the magnetic field is stabilized by temperature and an NMR magnetometer is used only to measure the resulting magnetic field. It takes several hours to warm up the magnet to working temperature, so the standard must be turned on at least 6 hours before measurement. But it also depends on the ambient temperature. When the standard is heated to operating temperature, it is switched off for a few minutes and heated again to operating temperature after it is switched on again.

NMR magnetometer circuit

The circuit consists of a microcomputer that controls the measurement and digitizes the NMR signal, a switch with $\lambda/4$ line, an NMR probe, and a receiver. The measurement starts with the microcomputer sending a RF pulse which, after being amplified by a power amplifier, switches the switch to the appropriate position and excites a sample of hydrogen nuclei (water, oil, fat, etc.) in the NMR probe. When returning

to rest, the sample emits a signal containing information about the instantaneous value of the permanent magnet's magnetic field in its spectrum. The signal is directed by a switch to the receiver, where it is amplified and detected. It is then digitized in the microcomputer. The data is transmitted to the parent computer via Ethernet. The phase of the NMR data depends approximately linearly on the relative temperature. Therefore, the NMR sample is cooled to approximately room temperature. The cooling contributes to a high measurement accuracy.

Parameters

Working magnetic induction	0.47 Tesla
Slot between pole nozzles	20 mm
Working magnet temperature approx.	38.6 °C
Ambient temperature	17° - 28 °C
Sampling rate	3.90625 MS/s
Sampling interval	$T = 0.256 \cdot 10^{-6} s$
Number of time samples	$n = 16384$
Number of frequency samples	$N = 2^{22}$
K -th frequency sample	$\Delta\omega_{0K} = \frac{2\pi K}{NT} \pm \left(\frac{2\pi}{NT} \Delta K + \frac{2\pi K}{NT^2} \Delta T \right)$
Gyromagnetic ratio	$\gamma = 2,675153268 \cdot 10^8 s^{-1} Tesla^{-1}$
Magnetometer step:	

$$\frac{\Delta\omega_{0i}}{\gamma} = \frac{1}{\gamma} \cdot \left(\frac{2\pi}{NT} \pm \left(\frac{2\pi}{NT} \cdot 0.5 + \frac{2\pi}{NT} \cdot 10^{-4} \right) \right) =$$

$$= 1.37436 \cdot 10^{-7} \pm (6,87179 \cdot 10^{-8} + 1,37436 \cdot 10^{-11}) Tesla$$

$$\text{Relative error of the magnetometer is } \pm \left(\frac{\Delta K}{K} + \frac{\Delta T}{T} \right)$$

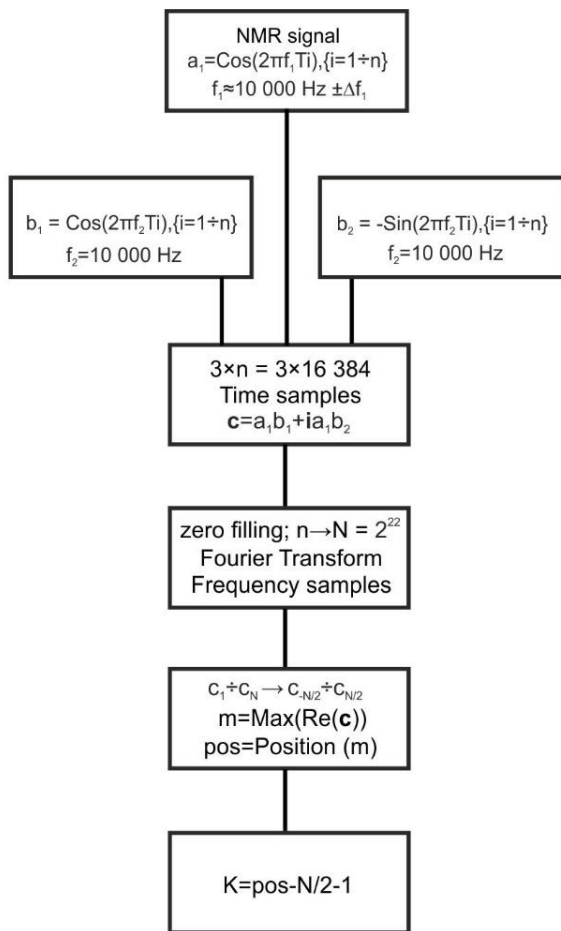
$$B_0 = \frac{1}{\gamma} \cdot \Delta\omega_{0K} = 0.47 \pm (1.09371 \cdot 10^{-8} + 0.00004) Tesla$$

K is an integer, it is the order of the frequency sample that has the largest size in the investigated spectrum.

Ideally, when the spectrum can be considered linear, $\Delta K = 0 \div 0.5$. Often the spectrum is not linear. In this case ΔK is calculated from adjacent samples and its value may be greater than 0.5 and K is not an integer. The relative error due to K also depends on the absolute value of K . Similarly, the relative error due to the sampling time interval T is the case. However, we know that frequencies and time intervals in computers are usually derived from quartz crystal oscillators. The relative accuracy of standard quartz crystals tends to be 10^{-4} and so we can also estimate the ratio $\frac{\Delta T}{T}$. The values of T and ΔT are known and do not change during the measurement, so this part of the error can be compensated quite easily. A more complicated situation is with an error due to K . It changes with the signal changes and can only be reduced by trying to determine K as accurately as possible or by choosing the measurement parameters so that K is as large as possible. If the spectrum is an even function of frequency, two values for K that are opposite in polarity, are obtained. Therefore, the receiver is supplemented with a logic algorithm that determines K polarity. Another way is to use a quadrature detector that provides a complex signal at the output from which K is obtained in the correct polarity. A computer simulation for calculating the frequency deviation can be found in the next paragraph.

Computer simulation: calculation of frequency deviation

The spectrum of a real function is an even function of frequency. For such a function, it is not possible to distinguish between positive and negative frequency deviation $\Delta\omega_0$. The problem is usually solved by transforming a real function into a complex function. The spectrum of a complex frequency function is not an even function. When a new device is constructed, a complex function with quadrature detector is created even before digitization. In this case, we were bound to the existing electronics, to which this modification also had to be adapted. The chosen solution was verified by a computer simulation, which is shown as a block diagram in Fig. 2. Obviously, the entire adjustment can be done in the software.



$K = -2013 \rightarrow +10\,738; \Delta f = K \cdot 1/NT = -1875 \rightarrow +10\,000 \text{ Hz}$
 $K = -19\,458 \rightarrow -10\,738; \Delta f = -K \cdot 1/NT - 2 \cdot f_2 = -1880 \rightarrow -10\,000 \text{ Hz}$

Fig. 2. Block diagram of the simulation of complex spectrum and frequency deviation calculation.

For simplicity, the NMR signal is simulated by a harmonic signal a_1 with a frequency of about $f_1 = 10,000 \pm \Delta f_1$ Hz. Since it is simulated by a computer, it is immediately digital. The signal a_1 is mixed with the signals b_1 and b_2 with a frequency of exactly $f_2 = 10,000$ Hz, but with a phase difference of $\pi/2$ ($\cos(\pi/2 + \alpha) = -\sin \alpha$). Both signals are in digital form. The number of samples is the same for all three

signals: $n = 16,384$. This creates a complex digital signal c . To achieve a higher resolution, the signal c is interpolated. The zero filling method is used, in which zeros are added to n time samples, so that the number of samples of the signal c increases to $N = 2^{22}$ samples. Mixing signals with a balanced mixer is mathematically a multiplication of signals. The signal c is processed by a discrete Fourier transform and the resulting frequency samples are arranged in a symmetric form. The real and imaginary parts of the signal c (spectrum) are interesting in terms of its frequency analysis (they are not even). The typical real part near the maximum is shown in Fig. 3.

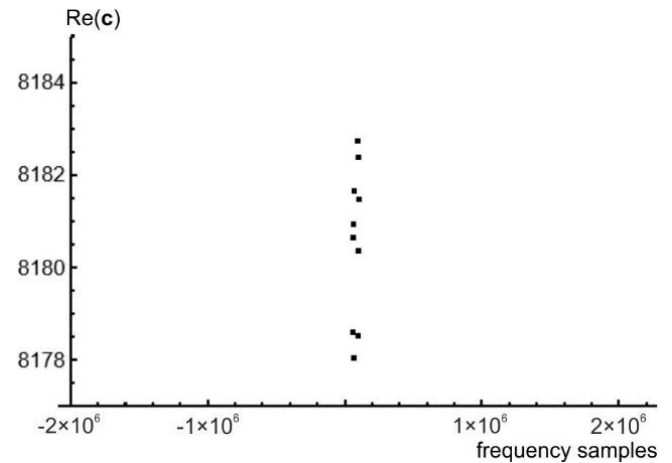


Fig. 3. Typical course of the real part of the complex spectrum near the maximum.

To calculate the strongest frequency sample, a real component was selected, the maximum signal $\text{Re}(c)$ and its position are important. This is sufficient to calculate the constant K from which the frequency deviation Δf is calculated. It is clear that its calculation is more complicated than in the case of an even spectrum, but such a result is more valuable. The value of $N = 2^{22}$ was chosen in terms of compatibility with other quantities obtained in the standard. The simulation was carried out with the interactive program Mathematica from Wolfram Research, for practice it is envisaged with a non-interactive program.

Without interpolation, the step of the magnetometer is $5.599 \cdot 10^{-6} T$, with interpolation it is $2.187 \cdot 10^{-8} T$. The described analysis calculates the number K from which the frequency deviation is determined using one of the two formulas (in Fig. 2). Which formula is used depends on the value of K . For comparison, an analysis with an imaginary component of the c spectrum was also performed, and the results were identical to the analysis of the real component. However, the calculation with the real component is simpler, more accurate, and more elegant. The described procedure is our original result. However, the quadrature detector and circuits with it are quite well known, so it is quite likely that other authors have come to a similar result in the past. The novelty could be in the software implementation of the circuits.

3. RESULTS

Mechanically, the standard consists of two cabinets connected by cables. The case, where most of the control circuits are located, is connected to the parent computer via Ethernet. This case also contains a microcomputer whose main task is to digitize the NMR signal. Signal processing and other activities are performed on a parent computer. If it is a laptop, it must not enter sleep mode, because this will interrupt the operation of the control program. A view of the benchmark from the front is shown in Fig. 4. The parent computer (laptop) is not visible in the picture. However, the cooling of the NMR sample is visible on the magnet case. On the case with the control electronics (including a microcomputer) there is a power switch. When it is set to the On position, a characteristic table appears on the display of the

parent computer, which contains the temperature data and the measured deviation of the magnetic field. It takes several minutes for the circuits to warm up to working temperatures, and for the desired result to appear on the display of the parent computer. This applies if the standard has already been switched On before and the magnet is heated. If this is not the case, the magnet must be heated to working temperature for the standard to signal a steady state, that is, usable values. The view of the standard from the rear is shown in Fig. 5. Again, the parent computer is not visible. The identically marked connectors on both parts of the magnetometer must be connected by appropriate cables. The tables on the display of the parent computer (Fig. 6 and Fig. 7) show the main parameters, both after stabilization and during system start-up in the Operation mode and in the Service mode.



Fig. 4. Benchmark from the front. The NMR sample cooling device is mounted on a permanent magnet housing.



Fig. 5. Benchmark from behind. Here is the vast majority of connectors and some controls. The corresponding connectors must be connected by dedicated cables.

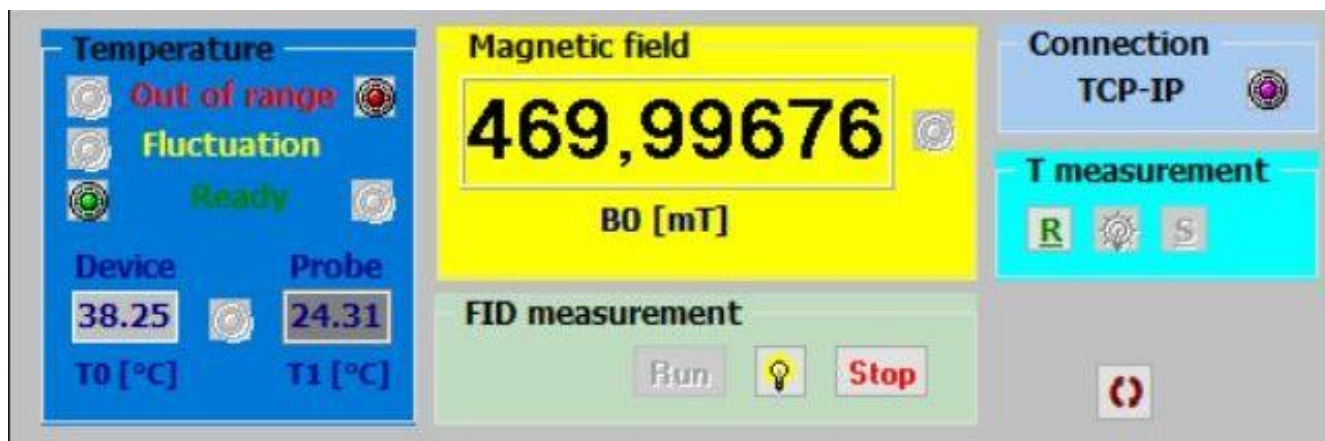


Fig. 6. Table on the display of the parent computer in the steady state. The resulting magnetic field can be gently adjusted by a designated element.

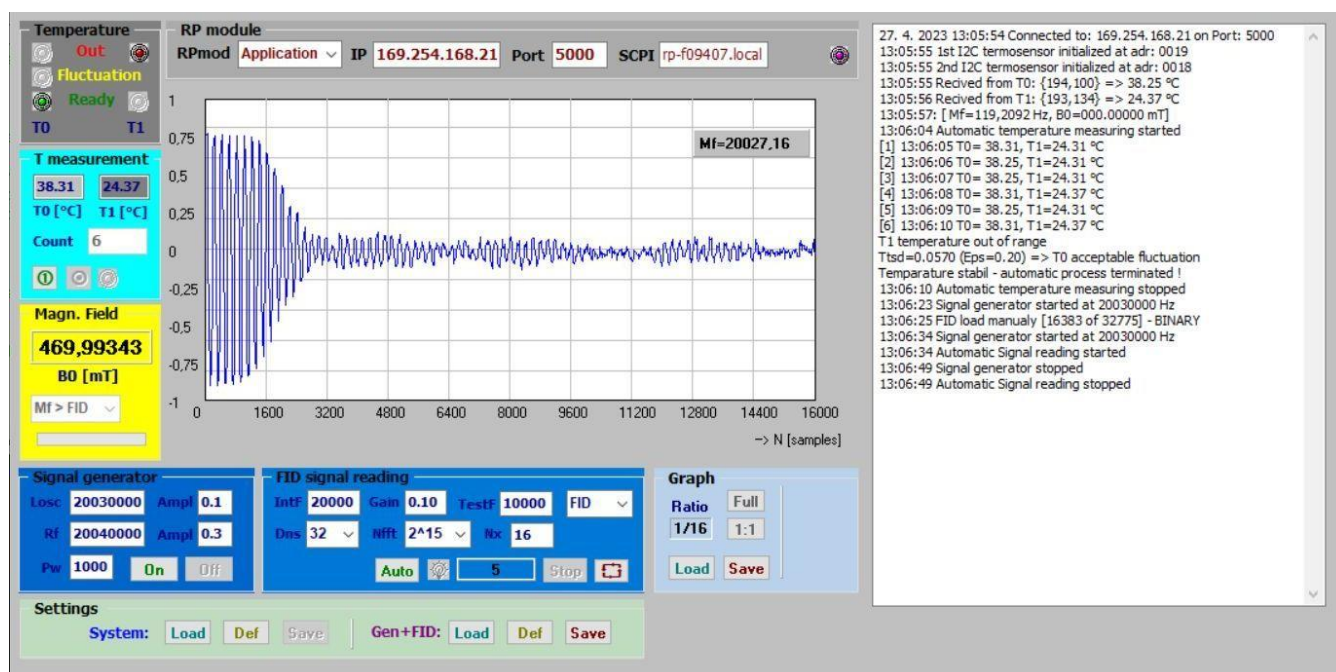


Fig. 7. Table on the display of the parent computer in the service mode.

4. DISCUSSION AND CONCLUSION

Describing all the details of this static magnetic field standard construction is far beyond the scope of this article. Therefore, the article focuses mainly on the NMR side of the structure, which we consider most important for the accuracy of magnetic field generation, and describes most of the other sides much more succinctly. There is a global description of the entire instrument, illustrated by a block diagram. The circuitry of the permanent magnet is described very briefly, using many elements from the original Minispec design. More attention is given to the NMR circuits, including a description of the magnetometer, which contains more original elements. Also interesting is the analysis of the measurement errors of the magnetometer, which provides an error signal for the magnetic field stabilizer. Mentioned is an algorithm that transforms even frequency deviation values

into a complete signal with the actual polarity of the frequency samples. However, a detailed description was not made. Instead, there is a computer simulation that simulates a quadrature detector and uses it to obtain a sequence of frequency samples with the correct polarity. Probably both methods are original and probably novel enough for an article in a corresponding publication. Pictures and brief descriptions of the resulting hardware and software are given as results. Circuits and devices not described in detail could also be topics of future publications. Probably this device will be a useful tool for scientific research.

ACKNOWLEDGMENT

This work was supported by the Scientific Grant Agency VEGA 2/0003/20, and VEGA 2/0004/23, and within the project of the Research and Development Agency No. APVV-19-0032.

REFERENCES

- [1] Brigham, E. O. (1974). *The Fast Fourier Transform*. Prentice-Hall, ISBN 9780133074963.
- [2] Čížek, V. (1981). *Discrete Fourier Transforms and their Applications*. Prague, Czech Republic: SNTL, ISBN 9780852748008. (in Czech)
- [3] Andris, P., Dermek, T., Gogola, D., Přibil, J., Frollo, I. (2022). Analysis of NMR signal for static magnetic field standard. *Measurement Science Review*, 22 (2), 81-85. <https://doi.org/10.2478/msr-2022-0010>
- [4] Sundramoorthy, S. V., Epel, B., Halpern, H. J. (2017). A pulse EPR 25 mT magnetometer with 10 ppm resolution. *Applied Magnetic Resonance*, 48 (8), 805-811. <https://doi.org/10.1007/S00723-017-0902-0>
- [5] Keller, P. (2011). NMR Magnetometers. *Magnetics Technology International*, 68-71.
- [6] Ulvr, M., Kupec, J. (2018). Improvements to the NMR method with flowing water at CMI. *IEEE Transaction on Instrumentation and Measurement*, 67 (1), 204-208. <https://doi.org/10.1109/TIM.2017.2756119>
- [7] Hoult, D. I., Richards, R. E. (1976). The signal-to-noise ratio of the nuclear magnetic resonance experiment. *Journal of Magnetic Resonance*, 24 (1), 71-85. [https://doi.org/10.1016/0022-2364\(76\)90233-X](https://doi.org/10.1016/0022-2364(76)90233-X)
- [8] Hoult, D. I., Lauterbur, P. C. (1979). The sensitivity of the zeugmatographic experiment involving human samples. *Journal of Magnetic Resonance*, 34 (2), 425-433. [https://doi.org/10.1016/0022-2364\(79\)90019-2](https://doi.org/10.1016/0022-2364(79)90019-2)
- [9] Weis, J., Ericsson, A., Hemmingsson, A. (1999). Chemical shift artifact-free microscopy: spectroscopic microimaging of the human skin. *Magnetic Resonance in Medicine*, 41 (5), 904-908. [https://doi.org/10.1002/\(sici\)1522-2594\(199905\)41:5%3C904::aid-mrm8%3E3.0.co;2-4](https://doi.org/10.1002/(sici)1522-2594(199905)41:5%3C904::aid-mrm8%3E3.0.co;2-4)
- [10] Marcon, P., Bartusek, K., Dokoupil, Z., Gescheidtova, E. (2012). Diffusion MRI: Mitigation of magnetic field inhomogeneities. *Measurement Science Review*, 12 (5), 205-212. <https://sciendo.com/article/10.2478/v10048-012-0031-8>
- [11] Bartusek, K., Dokoupil, Z., Gescheidtova, E. (2007). Mapping of magnetic field around small coil using the magnetic resonance method. *Measurement Science and Technology*, 18 (7), 2223-2230. <https://doi.org/10.1088/0957-0233/18/7/056>
- [12] Nešpor, D., Bartusek, K., Dokoupil, Z. (2014). Comparing saddle, slotted-tube and parallel-plate coils for magnetic resonance imaging. *Measurement Science Review*, 14 (3), 171-176. <https://doi.org/10.2478/msr-2014-0023>
- [13] Latta, P., Gruwel, M. L., Volotovskyy, V., Weber, M. H., Tomanek, B. (2008). Single-point imaging with a variable phase encoding interval. *Magnetic Resonance Imaging*, 26 (1), 109-116. <https://doi.org/10.1016/j.mri.2007.05.004>
- [14] Witkovsky, V., Frollo, I. (2020). Measurement science is the science of sciences - there is no science without measurement. *Measurement Science Review*, 20 (1), 1-5. <https://doi.org/10.2478/msr-2020-0001>

Received January 30, 2023

Accepted June 12, 2023